Process Biochemistry xxx (xxxx) xxx–xxx

Contents lists available at ScienceDirect

Process Biochemistry

journal homepage: www.elsevier.com/locate/procbio

Ether-functionalized ionic liquids for nonaqueous biocatalysis: Effect of different cation cores

Hua Zhao*, Naphatsawan Kanpadee, Chanida Jindarat

Department of Chemistry and Biochemistry, University of Northern Colorado, Greeley, CO 80639, USA

ARTICLE INFO

Keywords:
Biocatalysis
Ionic liquid
Lipase
Transesterification
Ring-opening polymerization
Enzyme activity
Thermal stability

ABSTRACT

Ether-functionalized ionic liquids (ILs) usually have low viscosities, and can be designed to be compatible with enzymes. However, there is a lack of understanding of the effect of different ether-functionalized structures on the enzyme activity. We systematically evaluated new ether-functionalized ILs carrying different cation cores (pairing with Tf_2N^- anions) in two Novozym 435-catalyzed reactions: (1) the transesterification of ethyl sorbate with 1-propanol at 50 °C; (2) the ring-opening polymerization (ROP) of ε-caprolactone at 70 °C. The lipase showed different activities: in the first reaction, $[CH_3OCH_2CH_2\text{-}Et_3N][Tf_2N]$ and $[CH_3OCH_2CH_2\text{-}Py][Tf_2N]$ gave the highest reaction rates; in the second reaction, $[CH_3OCH_2CH_2\text{-}PBu_3][Tf_2N]$ produced the highest molecular mass (M_w up to 25,400 Da). The lipase's thermal stability in $[CH_3OCH_2CH_2\text{-}Et_3N][Tf_2N]$ was found much higher than that in *t*-butanol. The fluorescence spectra of free lipase (excited at 280 nm) in these ILs reveal that the wavelength of the maximum emission peak occurred at 314 nm for both $[CH_3OCH_2CH_2PBu_3][Tf_2N]$ and $[CH_3OCH_2CH_2PEt_3][Tf_2N]$, which matched closely with that (313 nm) in aqueous phosphate buffer (pH 7.5, 20 mM), while other ether-functionalized ILs led to various degrees of red shifts. In summary, the lipase activity is not only dependent on the IL structure, but also on the substrate and other reaction conditions.

1. Introduction

Enzymatic reactions are often reversible, and thus an enzyme can synthesize or decompose the substrate molecules depending on the reaction conditions. Reaction medium is one of the most critical factors that can shift the reaction direction. As an example, hydrolases (such as proteases, lipases and cellulases) catalyze the hydrolysis (i.e. decomposition) of different substrates (e.g. peptides, lipids, and cellulose respectively) in aqueous media; on the other hand, these reactions are reversed (i.e. synthesis) in nonaqeuous solvents including organic solvents, supercritical fluids, and ionic liquids (ILs) [1–3]. However, the enzyme activities in nonaqueous organic solvents are usually lower by several magnitudes than those in aqueous solutions. For instance, the proteases α-chymotrypsin and subtilisin in anhydrous octane showed 10^4–10^5 times lower activities than in water [4]. The underlying mechanism is not fully understood, but several important parameters have been discussed including the substrate diffusion, accessibility of enzyme's active site, structural changes of enzyme molecules, energetics of substrate desolvation and transition state stabilization, conformational mobility, and pH optimization [5].

Ionic liquids (ILs) are alternative nonaqueous media (vs. conventional organic solvents) for biocatalysis due to their designable structures and tunable properties [6–11]. To mimic the water-like environment for favorable enzyme-solvent interactions, different versions of hydroxy- or ether-/glycol-functionalized ILs have been developed for a variety of enzymatic reactions. A number of commercial glycol-grafted tetraammonium-based ILs were evaluated by the Xu group [12–17] as reaction media for the enzymatic glycerolysis; particularly, Ammoeng 100 (known as $[CPMA][MeSO_4]$[1]) and Ammoeng 102 were able to dissolve triglycerides and afforded high lipase activities during glycerolysis [13,14]; in addition, trioctylmethylammonium bis(trifluoromethylsulfonyl)imide ($[TOMA][Tf_2N]$) and its mixture with Ammoeng 102 led to effective enzymatic glycerolysis [16–18]. Higher transesterification activities were reported in $[CPMA][MeSO_4]$ (vs. non-functionalized ILs) for both free and immobilized *Candida antarctica* lipase B (CALB); however, lipases from *Thermomyces lanuginosus* (TLL) and *Rhizomuncor miehei* (RML) became less active in $[CPMA][MeSO_4]$ [19]. Higher activities of alcohol dehydrogenase were observed by the Kroutil group [20] in hydroxy-functionalized ILs than in ordinary ILs even when the IL concentrations were up to 50–90% (v/v). An aqueous two-phase system (ATPS) was constructed from Ammoeng 110, and was used to purify active enzymes (two alcohol dehydrogenases); the Kragl

* Corresponding author.
E-mail address: hua.zhao@unco.edu (H. Zhao).

[1] From the name of cocosalkyl pentaethoxy methylammonium methylsulfate.

https://doi.org/10.1016/j.procbio.2019.03.018
Received 9 February 2019; Received in revised form 9 March 2019; Accepted 19 March 2019

group found the IL could stabilize the enzymes while dissolving more hydrophobic substrates [21]. Tetrakis(2-hydroxyethyl)ammonium triflouromethanesulfonate was prepared by Das et al [22], and was found highly compatible with horseradish peroxidase than methanol (10-fold more active) and conventional ILs (30–240-fold more active). An ether-functionalized phosphonium, 2-methoxyethyl(tri-*n*-butyl)phosphonium bis(trifluoromethylsulfonyl)imide ($[MeOCH_2CH_2\text{-}Bu_3P][Tf_2N]$) was synthesized by the Itoh group [23], and this IL enabled a faster reaction rate than diisopropyl ether for the transesterification of secondary alcohols catalyzed by lipase PS. Another group [24] reported the use of two functionalized ILs (i.e. $[C_2OHmim][PF_6]$ and $[C_5O_2mim][PF_6]$) for the esterification of glycerol with sinapic acid catalyzed by feruloyl esterase, and obtained high yields (up to 72.5% and 76.7% respectively in these two ILs). The Yuan group [25] synthesized several ether-grafted imidazolium-type ILs, and reported that 1-(3-ethoxypropyl)-2,3-dimethylimidazolium bis(trifluoromethylsulfonyl)imide enabled 99% enantioselectivity and 50% conversion for the Novozym534-catalyzed transesterification of *rac*-1-phenylethanol with vinyl acetate. Fan et al. [26] found that a hydroxy-containing IL, *N*-methyl-*N*-(3-hydroxypropyl)pyrrolidinium bis(trifluoromethylsulfonyl)imide was more effective than organic solvents (e.g. *n*-hexane and *t*-butanol) and non-functionalized ILs for improving the biodiesel yield during the lipase-catalyzed transesterification of soybean oil with methanol. The same group [27] also demonstrated that hydroxy-containing imidazolium ILs with short alky chains [such as 1-(3-hydroxypropyl)-3-methylimidazolium bis(trifluoromethylsulfonyl)imide] could enhance the lipase activity for the Michael addition synthesis of warfarin from 4-hydroxycoumarin and benzylideneacetone. The Itoh group [28] coated *Burkholderia cepacia* lipase by pyridinium-based ILs carrying cetyl-PEG_{10} sulfate (a glycol-functionalized anion), and reported that these enzyme preparations led to high reaction rates and enantioselectivities for the transesterification of a variety of secondary alcohols.

Previously, our group designed a series of hydroxy- or ether-functionalized imidazolium- and alkylammonium-based ILs containing the acetate anion [29,30]. We reported that several ether-functionalized ILs could dissolve a variety of substrates (e.g. cellulose, sugars, ascorbic acid, amino acids, betulinic acid, fatty acids, and triglycerides) that are not typically soluble in common organic solvents; meanwhile, these ILs enabled reasonably high enzymatic activities in several lipase-catalyzed transesterification reactions [29,31,32]. The hydrophobic versions (carrying Tf_2N^- anions) of three ether-functionalized ILs containing 10–15% (v/v) water led to high synthetic activities and selectivities in the subtilisin-catalyzed transesterification of *N*-acetyl-L-phenylalanine ethyl ester with 1-propanol [33]. Our recent study [34] synthesized several new ether-functionalized ILs (based on phosphonium, imidazolium, pyridinium, alkylammonium, and piperidinium cations) carrying Tf_2N^- anions for the high-temperature enzymatic polymerization reactions (70 °C for the polymerization of ε-caprolactone, and 130 °C for the polymerization of L-lactide). However, there is no systematic comparison of how different ether-functionalized ILs affect the enzyme stabilization, and a lack of mechanistic discussion of the IL structure-enzyme activity relationship. This study intends to prepare a series of IL cation cores functionalized by ether-chains, and then systematically evaluate how these tailored structures stabilize the enzyme. To achieve this objective, we screened these custom-made ILs by two CALB-catalyzed synthetic reactions: the transesterification of ethyl sorbate with 1-propanol at 50 °C, and the ring-opening polymerization (ROP) of ε-caprolactone at 70 °C. We further probed the CALB-IL interactions by fluorescence emission spectra for a molecular-level view of enzyme stabilization in different types of solvents. Our results provide general guidance for designing enzyme-compatible ether-functionalized ILs.

2. Materials and methods

2.1. Materials

Free *Candida antarctica* lipase B (CALB), which is a recombinant from *Aspergillus oryzae* (catalog #62288, Lot# BCBP3380V), and Novozym 435, known as CALB immobilized on acrylic resin (Catalog #L4777, Lot # SLBW1544 and # SLBP0766V) were purchased from Sigma-Aldrich (St. Louis, MO). 2-Bromoethyl methyl ether was the product of BeanTown Chemical (Hudson, NH), and lithium bis(trifluoromethylsulfonyl)imide ($Li[Tf_2N]$) was the product of Matrix Scientific (Columbia, SC), both of which were supplied by VWR (Radnor, PA). 1-Bromo-2-(2-methoxyethoxy)ethane, 1-(2-bromoethoxy)-2-(2-methoxyethoxy)ethane, ε-caprolactone, 2-chloroethyl ethyl sulfide, and 2-chloroethyl phenyl sulfide were provided by TCI America (Portland, OR). 1-Butyl-3-methylimidazolium bis(trifluoromethylsulfonyl)imide ($[BMIM][Tf_2N]$, synthesis grade) and 1-butyl-3-methylimidazolium hexafluorophosphate ($[BMIM][PF_6]$, high purity) were produced by Merck KGaA (EMD Millipore Corporation, Billerica, MA) and supplied by VWR (Radnor, PA).

2.2. Preparation of several ether-functionalized ILs

Ether-functionalized ILs based on phosphonium, imidazolium, pyridinium, alkylammonium, and piperidinium cations (see Table 1) were recently prepared and characterized in our laboratory [34]: 2-methoxyethyl-triethylphosphonium bis(trifluoromethylsulfonyl)imide ($[MeOCH_2CH_2\text{-}PEt_3][Tf_2N]$), 2-methoxyethyl-tributylphosphonium bis(trifluoromethylsulfonyl)imide ($[MeOCH_2CH_2\text{-}PBu_3][Tf_2N]$), 2-methoxyethyl-tributylphosphonium bis(pentafluoroethanesulfonyl)imide ($[MeOCH_2CH_2\text{-}PBu_3][beti]$), (2-methoxyethoxy)ethyl-tributylphosphonium bis(trifluoromethylsulfonyl)imide ($[Me(OCH_2CH_2)_2\text{-}PBu_3][Tf_2N]$), (2-(2-methoxyethoxy)ethoxy)ethyl-tributylphosphonium bis(trifluoromethylsulfonyl)imide ($[Me(OCH_2CH_2)_3\text{-}PBu_3][Tf_2N]$), 1-ethyl-3-(2-methoxyethyl)imidazolium bis(trifluoromethylsulfonyl)imide ($[MeOCH_2CH_2\text{-}Im\text{-}Et][Tf_2N]$), *N*-(2-methoxyethyl)pyridinium bis(trifluoromethylsulfonyl)imide ($[MeOCH_2CH_2\text{-}Py][Tf_2N]$), *N*-(2-methoxyethyl)-*N*-methylpiperidinium bis(trifluoromethylsulfonyl)imide ($[MeOCH_2CH_2\text{-}Pip\text{-}Me][Tf_2N]$). 2-(Ethylmercapto)ethyl-tributylphosphonium bis(trifluoromethylsulfonyl)imide ($[CH_3CH_2SCH_2CH_2\text{-}PBu_3][Tf_2N]$) and 2-(phenylmercapto)ethyl-tributylphosphonium bis(trifluoromethylsulfonyl)imide ($[PhSCH_2CH_2\text{-}PBu_3][Tf_2N]$) were prepared followed the same method [34] by refluxing 2-chloroethyl ethyl sulfide or 2-chloroethyl phenyl sulfide with tributylphosphine first, followed by the anion exchange from Cl^- to Tf_2N^-.

$[CH_3CH_2SCH_2CH_2\text{-}PBu_3][Tf_2N]$. ^{1}H-NMR (400 MHz, $CDCl_3$, [ppm]) δ = 0.97 (9H, m, $3CH_3CH_2CH_2CH_2$-), 1.28 (3H, t, CH_3CH_2S-), 1.52 (12H, m, $3CH_3CH_2CH_2CH_2$-), 2.21 (6H, m, $3CH_3CH_2CH_2CH_2$), 2.50 (2H, m, -SCH_2CH_2-P), 2.63 (2H, m, CH_3CH_2S-), 2.81 (2H, m, -SCH_2CH_2-P). ^{13}C-NMR (101 MHz, $CDCl_3$, [ppm]) δ = 13.20, 13.48, 14.23, 18.63, 19.09, 19.18, 19.64, 23.22, 23.26, 23.42, 23.47, 23.66, 23.81, 23.86, 24.01, 26.23, 118.21, 121.40.

$[PhSCH_2CH_2\text{-}PBu_3][Tf_2N]$. ^{1}H-NMR (400 MHz, $CDCl_3$, [ppm]) δ = 0.94 (9H, m, $3CH_3CH_2CH_2CH_2$-), 1.43 (12H, m, $3CH_3CH_2CH_2CH_2$-), 2.16 (6H, m, $3CH_3CH_2CH_2CH_2$), 2.47 (2H, m, -SCH_2CH_2-P), 3.18 (2H, m, -SCH_2CH_2-P), 7.28–7.36 (5H, m, C_6H_5S-). ^{13}C-NMR (101 MHz, $CDCl_3$, [ppm]) δ = 13.20, 13.62, 18.47, 18.94, 23.31, 23.36, 23.63, 23.67, 23.71, 23.79, 24.17, 24.32, 26.31, 26.36, 27.07, 27.72, 118.26, 121.46, 127.75, 129.24, 129.66, 130.52, 132.99.

Table 1
Enzymatic transesterification of ethyl sorbate with 1-propanol[a].

Trial	Solvent	Solvent water content (wt%) [b]	Dynamic viscosity at 30 °C (mPa s) [c]	Enzyme activity (μmol min^{-1} g^{-1} CALB)	Selectivity
1	*t*-butanol	0.02	4.31 (25 °C) [39]	**7.38**	> 99%
2	*t*-butanol	0.41	–	6.12	> 99%
3	*N*,*N*-dimethylacetamide	0.01	1.927 (25 °C) [39]	2.38	> 99%
4	[BMIM][PF_6]	0.01	205.8	3.87	86.6
5	[BMIM][Tf_2N]	0.01	41.4	**5.12**	> 99%
6	[BMIM][BF_4]	0.03	85 [65]	3.41	> 99%
7	[BMIM][dca]	0.05	26 [66]	0.23	> 99%
8	[$CH_3OCH_2CH_2$-PBu_3][Tf_2N]	0.01	122.5	1.77	93.5
9	[$CH_3OCH_2CH_2$-PBu_3][Tf_2N]	0.02	–	0.94	> 99%
10	[$CH_3(OCH_2CH_2)_2$-PBu_3][Tf_2N]	0.02	95.5	0.53	> 99%
11	[$CH_3(OCH_2CH_2)_3$-PBu_3][Tf_2N]	0.01	79.8	0.21	98.3
12	[$CH_3OCH_2CH_2$-PBu_3][beti]	0.02	163.4	1.03	> 99%
13	[$CH_3OCH_2CH_2$-PEt_3][Tf_2N]	0.01	36.0	**4.97**	> 99%
14	[$CH_3OCH_2CH_2$-Im-Et][Tf_2N]	0.01	33.1	3.27	99.2
15	[$CH_3OCH_2CH_2$-Py][Tf_2N]	0.01	44.5	**6.08**	> 99%
16	[$CH_3OCH_2CH_2$-Et_3N][Tf_2N]	0.01	61.4	**6.57**	> 99%
17	[$CH_3OCH_2CH_2$-Pip-Me][Tf_2N]	0.01	84.2	4.13	> 99%
18	[$CH_3OCH_2CH_2$-SMe_2][Tf_2N]	0.02	47.1 [d]	4.09	90.4
19	[$CH_3(OCH_2CH_2)_2$-SMe_2][Tf_2N]	0.03	–	2.55	> 99%
20	[$CH_3(OCH_2CH_2)_2$-SMe_2][Tf_2N]	0.01	91.3 [e]	2.39	> 99%
21	[$CH_3(OCH_2CH_2)_3$-SMe_2][Tf_2N]	0.02	111.3	**5.13**	99.5
22	[$C_6H_5SCH_2CH_2$-PBu_3][Tf_2N]	0.02	199.2	0.58	87.0
23	[$CH_3CH_2SCH_2CH_2$-PBu_3][Tf_2N]	0.04	206.4	0.039	> 99%

Note: [a] The enzymatic reaction between ethyl sorbate (5 mM) and 1-propanol (0.67 M) was performed in 1.0 mL solvent catalyzed by 20 mg Novozym 435 at 50 °C. [b] The water contents were determined by the coulometric Karl Fischer titration at 22 °C using Hydranal® Coulomat AG as the analyte. [c] The viscosity data at 30 °C were acquired by an Anton Paar SVM 3000 viscometer. [d] One literature reported 46.84 mPa s at 25 °C. [e] One literature reported 33.10 mPa s at 25 °C.

2.3. Preparation of ether-functionalized sulfonium-based ILs

A literature method [35] was slightly modified. Bromoglycol (1.0 eq.) was added dropwise into an aqueous solution of sodium thiomethoxide (21 wt%, 1.1 molar equiv.). The reaction mixture was covered by an aluminum foil and cooled in an ice bath for 24 h. Iodomethane (1.5 molar equiv.) was added dropwise to the reaction mixture (containing 1.0 equiv. glycol thioether), and the biphasic mixture was stirred at room temperature for 24 h. Into the reaction mixture, lithium bis(trifluoromethylsulfonyl)imide (Li[Tf_2N], 1.05 molar equiv.) dissolved in deionized water was added dropwise at room temperature. A cloudy mixture formed instantly. The mixture was continuously stirred for 20 min. After sitting for 2 h for the phase separation, the IL layer at the bottom was separated and dissolved in dichloromethane, which was thoroughly rinsed with deionized water three times. The silver nitrate test of the aqueous layer indicated the absence of halides. The rinsed IL was further washed by diethyl ether two times, and then dried in a vacuum oven (25 mmHg, 80 °C) for seven days. ^{1}H and ^{13}C NMR confirmed the structure and purity of the ILs.

2-Methoxyethyl-dimethylsulfonium bis(trifluoromethylsulfonyl)imide ([$MeOCH_2CH_2$-SMe_2][Tf_2N]). ^{1}H-NMR (400 MHz, $CDCl_3$, [ppm]) δ = 2.92 (6H, m, 2CH_3S-), 3.90 (3H, m, CH_3OCH_2CH_2S-), 3.51 (2H, m, $CH_3OCH_2CH_2$S-), 3.83 (2H, m, $CH_3OCH_2CH_2$S-). ^{13}C-NMR (101 MHz, $CDCl_3$, [ppm]) δ = 25.86, 44.19, 58.94, 66.43, 118.14, 121.32.

(2-Methoxyethoxy)ethyl-dimethylsulfonium bis(trifluoromethylsulfonyl) imide ([$Me(OCH_2CH_2)_2$-SMe_2][Tf_2N]). ^{1}H-NMR (400 MHz, $CDCl_3$, [ppm]) δ = 2.95 (6H, m, 2CH_3S-), 3.36 (3H, s, -$SCH_2CH_2OCH_2CH_2OCH_3$), 3.54 (4H, m, -$SCH_2CH_2OCH_2CH_2OCH_3$), 3.68 (2H, m, -$SCH_2CH_2OCH_2CH_2OCH_3$), 3.97 (2H, m, -$SCH_2CH_2OCH_2CH_2OCH_3$). ^{13}C-NMR (101 MHz, $CDCl_3$, [ppm]) δ = 25.72, 26.10, 44.26, 58.61, 65.04, 70.38, 71.22, 118.09, 121.27.

(2-(2-Methoxyethoxy)ethoxy)ethyl- dimethylsulfonium bis(trifluoromethylsulfonyl)imide ([$Me(OCH_2CH_2)_3$-SMe_2][Tf_2N]). ^{1}H-NMR (400 MHz, $CDCl_3$, [ppm]) δ = 2.95 (6H, s, 2CH_3S-), 3.35 (3H, s, -$SCH_2CH_2OCH_2CH_2OCH_2CH_2OCH_3$), 3.54 (4H, m, -$SCH_2CH_2OCH_2CH_2OCH_2CH_2OCH_3$), 3.62 (4H, m, -$SCH_2CH_2OCH_2CH_2OCH_2CH_2OCH_3$), 3.68 (2H, m, -$SCH_2CH_2OCH_2CH_2OCH_2CH_2OCH_3$), 3.97 (2H, m, -$SCH_2CH_2OCH_2CH_2OCH_2CH_2OCH_3$). ^{13}C-NMR (101 MHz, $CDCl_3$, [ppm]) δ = 25.82, 44.23, 58.76, 65.11, 69.82, 70.09, 70.44, 71.54, 118.08, 121.27.

2.4. Enzymatic transesterification of ethyl sorbate with 1-propanol

In a typical setup, 50 μL of 1-propanol containing 100 mM ethyl sorbate were mixed with 1.0 mL of IL in a capped glass vial. The final concentrations of ethyl sorbate and 1-propanol were 5 mM and 0.67 M, respectively. Following the addition of 20 mg Novozym 435, the reaction mixture was gently agitated at 50 °C in an oil bath. Periodically (every 15 min for the first hour), an aliquot (50 μL) of the mixture was withdrawn and diluted with 1.0 mL methanol. After centrifuging for 2 min, the clear supernatant was injected into a HPLC. The concentration of propyl sorbate was calculated from its integrated area against the standard curve for ethyl sorbate. As Novozym 435 can potentially leach trace amounts of sorbic acid and sorbate ester [32], control experiments were conducted without the addition of substrate (ethyl sorbate) but with 50 μL of 1-propanol. Therefore, all activities reported were the net activities after subtracting the control rates. LC-20AD Shimadzu HPLC equipped with a SPD-20A UV–vis dual-wavelength detector and an auto-sampler was used to analyze the reaction mixtures. The column employed was a Phenomenex® Kinetex C18 column (100 mm × 4.6 mm, particle size 2.6 mm). The flow rate was set at 1.0 mL min^{-1}. The isocratic eluent consisted of 60 vol% methanol and 40 vol% water containing 1 vol% acetic acid; the UV detection wavelength was set at 258 nm.

2.5. Enzymatic ROP of ε-caprolactone

ε-Caprolactone (0.5 g; density of 1.03 g/mL) was mixed with 0.25 mL of solvent and 100 mg of Novozym 435 in a reaction vial. After capping the viral, the reaction mixture was stirred (210 rpm) at 70 °C in an oil bath. After 48 h, the mixture was removed from the oil bath and allowed to cool to room temperature, followed by the addition of 2.0 mL of $CDCl_3$ to dissolve the polyester under stirring. To analyze the sample by ^{1}H NMR, an aliquot (50 μL) was taken from the mixture and diluted with 1.0 mL of $CDCl_3$; the diluted sample mixture was centrifuged. To analyze the sample by GPC, an aliquot (50 μL) was taken

from the reaction mixture and diluted with 1.0 mL THF, followed by a centrifugation before the GPC injection. To collect the solid product, chloroform was evaporated first and ice-cold methanol was added to precipitate the polymer, followed by the separation of solid from liquid using centrifugation or vacuum filtration. The polyester product was dried in air for 24 h.

The mass of isolated/dried product was divided by the mass of ε-caprolactone (0.5 g) to give the polyester yield. The ε-caprolactone conversion was calculated from the ^{1}H NMR spectrum (Bruker Avance II 400 MHz NMR) by using the integrated peak areas of the methylene groups next to the carbonyl group within ε-caprolactone (CL, 4.23 ppm) and poly(ε-caprolactone) (PCL, 4.07 ppm) [36]. The mass-average molecular mass (M_w) and polydispersity index (PDI = M_w/M_n) of the polymer were measured by a GPC (LC-20AD Shimadzu HPLC) equipped with SPD-20A UV–vis dual-wavelength detector operated at 210 nm, and two Agilent PLgel MIXED-B (10 μm, 300 × 7.5 mm) columns eluted with 1.0 mL/min THF at 30 °C [37]. The calibration curve was established by polystyrene standards with 570 to 62,500 (M_w) [38].

2.6. Fluorescence emission of free CALB in ILs

All fluorescence emission spectra were measured by a Hitachi F-2500 fluorescence spectrophotometer. The lipase solution was excited at 280 nm to observe the emission of tyrosine and tryptophan residues at about 300 nm. A lipase (free CALB) solution (10 μL, 20 mg/mL in pH 7.5, 20 mM phosphate buffer) was added into 1.0 mL of solvent (phosphate buffer, organic solvent, or IL) in a microcentrifuge tube. The tube was turned upside down several times to dissolve or disperse the aqueous enzyme in the solvent. The final lipase concentration was 0.2 mg/mL. The lipase solution was transferred to a quartz cuvette (1.0 mL volume). Fluorescence measurements were made at room temperature (22 °C) except that the measurement in *t*-butanol was determined at 30 °C (due to its low melting point of 25.8 °C [39]). The excitation monochromator slit was set to 5 nm, and the emission monochromator slit width was also set at 5 nm. The PMT voltage was controlled at 400 V and the response time was 0.08 s. The spectra were scanned from 250 to 400 nm at a rate of 300 nm/min. The emission spectrum of each solvent without the enzyme was also scanned at the same condition, which was subtracted from the CALB emission spectrum in the same solvent.

3. Results and discussion

We evaluated the lipase CALB's activities at two different temperatures through two synthetic reactions: a transesterification at a moderate temperature (50 °C), and a ring-opening polymerization at a higher temperature (70 °C).

3.1. Transesterification activities in different solvents

In contrast to conventional lipase-catalyzed transesterification assays (such as ethyl butyrate with 1-butanol), our group [32,40] previously developed a more sensitive reaction assay (see Scheme 1) between ethyl sorbate (a flavoring ingredient) and 1-propanol (or other sorbates with alcohols). This model reaction has several advantages including: (1) due to the highly conjugated double bonds, the reactant (ethyl sorbate), product (propyl sorbate), and byproduct (sorbic acid) can be easily detected at micromolar concentrations (μM) by a UV detector (e.g. at 258 nm) using the HPLC analysis; (2) the reaction is moderately fast and thus exhibits linear reaction rates during the first 1–2 hours under normal biocatalysis temperatures (30–50 °C).

Following this model reaction, we examined the initial reaction rates in a number of organic solvents and ILs catalyzed by Novozym 435 (see Table 1). It is well known that Novozym 435 contains about 10 wt % *Candida antarctica* lipase B (CALB) immobilized on the macroporous acrylic beads [41,42]. Therefore, we calculated the initial reaction rate (μmol min^{-1} g^{-1} CALB) based on the estimated CALB content (i.e. ~2 mg free CALB in 20 mg Novozym 435) while many studies used the total amount of CALB and acrylic beads to compute the reaction rate. In our study, most solvents contained extremely low water contents (e.g. 0.01–0.02 wt%). The reaction selectivity (synthesis vs hydrolysis) favored the transesterification reaction at low water contents (at least up to 0.41 wt% water in *t*-butanol, see trial 2 in Table 1). Most reactions in Table 1 achieved high selectivities of > 99%, and some variations in the selectivity seemed not correlated with the low water content. The initial rate in *t*-butanol with 0.02 wt% water (trial 1) was very high (7.38 μmol min^{-1} g^{-1} CALB), which is used as a reference for comparing the enzyme activity (although unlike ILs, *t*-butanol may not dissolve a variety of substrates and not be suitable for high-temperature enzymatic applications; see section 3.3). The initial rate decreased by 17% when the water content in *t*-butanol increased to 0.41 wt% (trial 2). When the water content varied between 0.01 wt% and 0.03 wt% (see trials 8 and 9, 19 and 20 in Table 1), there appeared no significant change in reaction rates. Under the low water content for a specific enzymatic reaction, the lipase activity mainly depends on the type of solvents. *N*,*N*-Dimethylacetamide (DMA) was less compatible with the enzyme (2.38 μmol min^{-1} g^{-1} CALB); three classic ILs [BMIM][PF_6] (3.87 μmol min^{-1} g^{-1} CALB), [BMIM][Tf_2N] (5.12 μmol min^{-1} g^{-1} CALB), and [BMIM][BF_4] (3.41 μmol min^{-1} g^{-1} CALB) were more lipase-activating than DMA. On the other hand, [BMIM][dca] showed a low enzyme activity (trial 7 in Table 1); we also observed that [BMIM][dca] even dissolved the immobilized CALB including the acrylic beads. It is well known that [BMIM][dca] is enzyme-denaturing due to the strong hydrogen-bonding capability of dicyanamide anions (dca^-) [29,31,43].

Ether-functionalized ILs displayed a wide range of biocompatibility with the lipase CALB (trials 8–23 in Table 1). All tributyl phosphonium ILs (trials 8–12 and 22–23) caused the lipase deactivation, resulting in initial rates below 2.0 μmol min^{-1} g^{-1} CALB. This could be due to the substrate ground-state stabilization by highly hydrophobic ILs carrying tributyl groups, not necessarily due to the hydrophobic interaction between tributyl groups and the protein leading to the enzyme inactivation (see the fluorescence spectrum in section 3.4); less hydrophobic triethyl phosphonium (trial 13) is four-fold more lipase-activating than the tributyl phosphonium analogue (trial 8). Surprisingly, longer glycol chains attached to tributyl phosphoniums (trials 8–11)

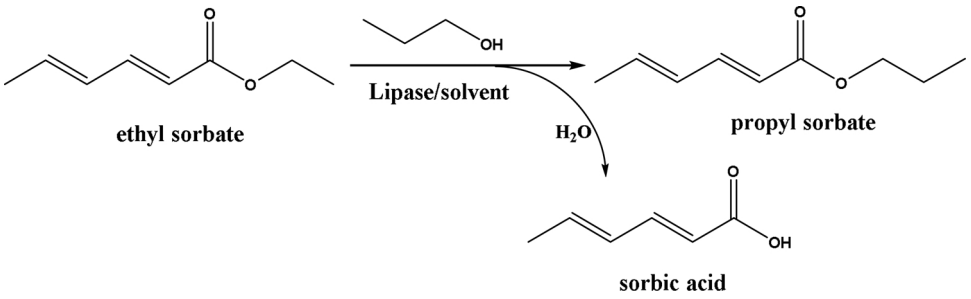

Scheme 1. Lipase-catalyzed transesterification of ethyl sorbate with 1-propanol.

resulted in even lower enzyme activities: ([$CH_3OCH_2CH_2$-PBu_3][Tf_2N] > [$CH_3(OCH_2CH_2)_2$-PBu_3][Tf_2N] > [$CH_3(OCH_2CH_2)_3$-PBu_3][Tf_2N]). However, this trend does not hold for the sulfonium ILs (trials 18–21), where the initial rates decreased in the order of [$CH_3(OCH_2CH_2)_3$-SMe_2][Tf_2N] > [$CH_3OCH_2CH_2$-SMe_2][Tf_2N] > [$CH_3(OCH_2CH_2)_2$-SMe_2][Tf_2N]. Therefore, the role of glycol chain is also cation-dependent. Different cation cores have drastic impact on their lipase compatibility in a decreasing order of triethylammonium (trial 16) > pyridinium (trial 15) > triethylphosphonium (trial 13) > piperidinium (trial 17), sulfonium (trial 18) > imidazolium (trial 14). In particular, high lipase activities at 50 °C were observed in these ILs: [$CH_3OCH_2CH_2$-Et_3N][Tf_2N] (6.57 μmol min^{-1} g^{-1} CALB), [$CH_3OCH_2CH_2$-Py][Tf_2N] (6.08 μmol min^{-1} g^{-1} CALB), [$CH_3(OCH_2CH_2)_3$-SMe_2][Tf_2N] (5.13 μmol min^{-1} g^{-1} CALB), [BMIM][Tf_2N] (5.12 μmol min^{-1} g^{-1} CALB), and [$CH_3OCH_2CH_2$-PEt_3][Tf_2N] (4.97 μmol min^{-1} g^{-1} CALB). The inclusion of ether groups in IL structures often leads to lower viscosities of the organic salts [31,44]. There is a poor correlation between the initial reaction rate and the Tf_2N^--based-IL viscosity (see Table 1), implying that the viscosity might play a role but not a determining factor.

3.2. High-temperature enzymatic polymerization of ε-caprolactone

The enzymatic ring-opening polymerization of ε-caprolactone was conducted at a higher temperature (70 °C) (see Table 2). Dimethylacetamide and ILs were used as co-solvents (0.25 mL with 0.5 g liquid ε-caprolactone) because higher solvent contents (such as 0.5 and 1.0 mL) usually led to lower molecular masses [34,45]. The polyester with high molecular mass appeared not soluble in these co-solvents, and the reaction mixture gradually solidified over time. Our earlier study suggested that the enzymatic polymerization could be largely affected by different batches of Novozym 435 and their water contents [45]. Higher water contents in the enzyme and the solvent resulted in lower molecular masses of polyesters [34,45]. Table 2 compared the data from two different batches of Novozym 435 (SLBP0766V and SLBW1544). The second enzyme batch (containing 0.68 wt% water as determined by Karl-Fischer titration) produced higher molecular masses (M_w) than the first batch (containing 1.09 wt% water) when comparing trial 10 and 2 (1.7 times higher) in [BMIM][PF_6], and trial 12 and 3 (1.3 times higher) in [$CH_3OCH_2CH_2$-PBu_3][Tf_2N]. Therefore, a conversion factor (1.3–1.7) should be considered when discussing data in trials 10–17 with trials 1–9 in Table 2. In general, the use of most co-solvents led to higher M_w than the solventless condition (trial 1 in Table 2). The incorporation of longer glycol chains to sulfoniums (trials 13–15), or thioether groups to phosphoniums (trials 16–17 vs 12) was unable to improve the molecular mass of poly(ε-caprolactone), which is consistent with our earlier findings where longer glycol chains were introduced to tributylphosphoniums for the synthesis of polylactide and poly(ε-caprolactone) [34]. The cationic headgroup of the IL imposed a significant impact on the polyester's M_w: phosphonium (trial 3) > piperidinium (trial 9), alkylammonium (trial 8) > pyridinium (trial 7), sulfonium (trial 13, after the enzyme batch conversion shown above) > imidazolium (trial 6). Overall, the phosphonium-based [$CH_3OCH_2CH_2$-PBu_3][Tf_2N] produced a relatively high molecular mass of polylactone with a high yield. This sequence of different cation cores is different from that concluded from the transesterification reaction above, suggesting that different ILs have profound effects on the lipase activation in different enzymatic reactions; different substrate stabilization, IL stability and temperatures could all be important factors. Polydispersity indexes (PDI) of poly(ε-caprolactone) fall in the range of 1.2–2.0 (Table 2), which are typically values for polyesters produced by enzymatic methods [46–50]. The molecular mass distribution in enzymatic ROP reactions can be attributed to the relative rates of initiation to propagation, and the possible chain transfer, termination, hydrolysis, and transesterification [50,51]. Due to such a complex reaction system, there is no apparent correlation between PDI and the type of solvents (Table 2).

3.3. Thermal stability of Novozym 435

Fig.1 compares the thermal stability of Novozym 435 after its incubation in *t*-butanol or [$CH_3OCH_2CH_2$-NEt_3][Tf_2N] for 24 h (or 48 h) at 50, 70 and 130 °C respectively. The remaining enzyme activity in *t*-butanol after 24 h at 50 °C was 17% (of its initial activity shown as trial 1 in Table 1) and only 1% after 24 h at 70 °C. On the contrary, the thermal stability of the lipase in [$CH_3OCH_2CH_2$-NEt_3][Tf_2N] after 24 h was much higher (86% at 50 °C, and 46% at 70 °C of its initial activity shown as trial 16 in Table 1) although Novozym 435 lost most of its activity after 24 h at 130 °C (1% remaining activity). A further incubation of the lipase in [$CH_3OCH_2CH_2$-NEt_3][Tf_2N] at 50 °C or 70 °C for 48 h led no further significant change of its enzyme activity (81% and 47% of the initial activity respectively). In conclusion, the thermal stability of Novozym 435 in [$CH_3OCH_2CH_2$-NEt_3][Tf_2N] is much higher than that in *t*-butanol, which makes the use of ILs for biocatalysis more advantageous than organic solvents like *t*-butanol. In general, ILs carrying anions of Tf_2N^-, PF_6^- and BF_4^- enable higher enzyme stabilities than those polar (e.g. 1-butanol and 1-propanol) or even less polar

Table 2
Enzymatic ROP of ε-caprolactone under different reaction conditions[a].

Trial	Novozym 435 batch	Solvent (water content)	Conversion (%)	Yield (%)	M_w (Da)[b]	PDI
1	SLBP0766V	no solvent	96.8	37	13,800	1.71
2	SLBP0766V	[BMIM][PF_6] (0.01 wt%)	87.8	**55**	**18,500**	1.94
3	SLBP0766V	[$CH_3OCH_2CH_2$-PBu_3][Tf_2N] (0.02 wt%)	96.9	**48**	**18,900**	1.59
4	SLBP0766V	[$CH_3OCH_2CH_2$-PBu_3][beti] (0.02 wt%)	52.1	15	9,100	1.19
5	SLBP0766V	[$CH_3(OCH_2CH_2)_2$-PBu_3][Tf_2N] (0.02 wt%)	70.1	30	14,300	1.35
6	SLBP0766V	[$MeOCH_2CH_2$-Im-Et][Tf_2N] (0.03 wt%)	95.7	42	12,300	1.60
7	SLBP0766V	[$MeOCH_2CH_2$-Py][Tf_2N] (0.03 wt%)	94.3	32	16,200	1.34
8	SLBP0766V	[$MeOCH_2CH_2$-Et_3N][Tf_2N] (0.03 wt%)	96.4	11	17,300	1.39
9	SLBP0766V	[$MeOCH_2CH_2$-Pip-Me][Tf_2N] (0.03 wt%)	96.1	11	18,100	1.69
10	SLBW1544	[BMIM][PF_6] (0.01 wt%)	98.6	38	31,400	1.55
11	SLBW1544	Dimethylacetamide (0.01 wt%)	99.0	**54**	**29,100**	1.75
12	SLBW1544	[$CH_3OCH_2CH_2$-PBu_3][Tf_2N] (0.02 wt%)	99.8	**56**	**25,400**	1.53
13	SLBW1544	[$CH_3OCH_2CH_2$-SMe_2][Tf_2N] (0.01 wt%)	99.0	**65**	**21,700**	1.89
14	SLBW1544	[$CH_3(OCH_2CH_2)_2$-SMe_2][Tf_2N] (0.02 wt%)	60.0	33	14,700	1.35
15	SLBW1544	[$CH_3(OCH_2CH_2)_3$-SMe_2][Tf_2N] (0.02 wt%)	71.2	37	19,000	1.46
16	SLBW1544	[$C_6H_5SCH_2CH_2$-PBu_3][Tf_2N] (0.02 wt%)	94.0	56	21,500	1.73
17	SLBW1544	[$CH_3CH_2SCH_2CH_2$-PBu_3][Tf_2N] (0.03 wt%)	95.9	55	14,800	1.65

[a] Note: general reaction conditions (unless otherwise noted): 0.5 g of ε-caprolactone, 0.25 mL of solvent, 100 mg of Novozym 435, gentle stirring (210 rpm) at 70 °C for 2 days. GPC-derived M_w values were based on results calibrated using polystyrene standards. Parts of the data (using Novozym 435 lot # SLBP0766V) were published in our earlier paper [34]. [b] Based on the GPC analysis.

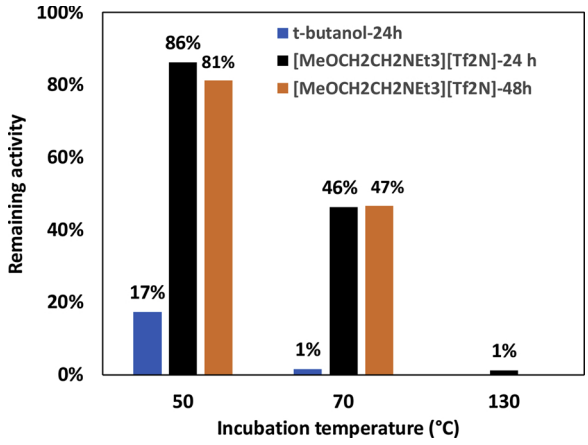

Fig. 1. Thermal stability of Novozym 435 in *t*-butanol and [$MeOCH_2CH_2$-Et_3N][Tf_2N]. Reaction conditions were as the following: 20 mg Novozym 435 incubated in 1.0 mL *t*-butanol or [$MeOCH_2CH_2$-Et_3N][Tf_2N] at a fixed temperature for 24 or 48 h. After cooling to room temperature, ethyl sorbate (50 μL 100 mM in 1-propanol) was added and the reaction mixture was immersed in an oil bath at 50 °C. The lipase activity was measured following the procedures in section 2.4.

organic solvents (e.g. *n*-hexane, dibutylether, and benzene), which can be explained by the *aprotic, non-coordinating, and neutral basicity nature* of the anions and their minimum perturbation of the protein (e.g. not having strong hydrogen bonding with the enzyme) [52–56]. In addition, short-chain-ether/glycol-functionalized ILs could improve the thermal stability of an enzyme even when the anion (e.g. acetate) was basic and forming hydrogen bonds [31]. Therefore, [$CH_3OCH_2CH_2$-NEt_3][Tf_2N] has combined these two advantages, resulting in a high thermal stability of Novozym 435. On the other hand, *t*-butanol is a polar aprotic solvent and miscible with water; molecular dynamics simulations suggest that *t*-butanol does not alert the substrate entrance and the binding pocket size of CALB, and also maintains hydrogen bonds between Ser105 and His224 residues (Ser105–His224–Asp187 as the catalytic triad in CALB's active site) [57], which explains the high lipase activity in *t*-butanol (trial 1 in Table 1). However, at higher temperatures (i.e. 50–70 °C), it appeared that CALB in Novozym 435 was detached from the polymer support over 24 h as we observed the solution became cloudy; we suspect that this solvent could have a strong interaction with the protein through hydrogen bonds, and/or strip off water from the enzyme.

3.4. Fluorescence emission spectra of CALB in ILs

CALB consists of 317 amino acid residues with a molecular mass of 33,273 Da, and has a Ser105–His224–Asp187 catalytic triad in its active site [58,59]. CALB has a high thermal stability, and may be active under temperatures as high as 100 °C [60]. As fluorophores in the protein, the tryptophan residues are selectively excited at 295 nm affording the emission maximum in water near 350 nm; the excitation of proteins at 280 nm leads to the energy absorption by both tryptophan and tyrosine (the emission maximum of tyrosine in water is near 303 nm) [61]. Therefore, following the excitation of CALB in phosphate buffer (pH 7.5, 20 mM) at 280 nm, the overall emission maximum of tryptophan and tyrosine residues was observed at 313 nm, whose fluorescence intensity was three times stronger than that being excited at 295 nm (Fig. S1 in the *Supporting Information*). Therefore, this study excited all other CALB samples at 280 nm, and all solvent emission signals were subtracted (Figs. S2–S22). The presence of water or *t*-butanol molecules in all samples gave a sharp peak of Raman scattering band at ~282 nm (interestingly, 0.2 mg/mL CALB in *t*-butanol led to > 34 times increase in peak intensity at 281 nm, see Fig. S2(a)). It is notable that many ILs themselves have strong emission signals at > 300 nm (see Figs. S4–S22 in the *Supporting Information*), particularly for imidazoliums (Figs. S4–S7, S17), piperidinium (Fig. S19), and multiple alkoxy groups (Figs. S12, S13, and S20–S22), which should all be subtracted from the enzyme-in-IL spectra. Usually, the changes in the maximal intensity of fluorescence and the red shift of the maximal emission wavelength indicate the protein denaturation [62].

The fluorescence spectrum of CALB in phosphate buffer (pH 7.5, 20 mM) was used as a reference of the native protein structure. The maximal intensity of fluorescence of CALB in *t*-butanol was higher than that in buffer (Fig. 2a). Visually, we observed a slightly turbid mixture formed; in turbid media, the light scattering and absorption often result in weaker fluorescence intensity, not a stronger intensity [63]. One possible explanation is that hydroxy groups of *t*-butanol interact with the protein surface through hydrogen-boning to cause the hydrophobic tyrosine and tryptophan residues to become more buried within the core of the protein, resulting in higher fluorescence intensity. Coincidentally, this corresponds to the highest CALB activity in Table 1. Aqueous droplets of CALB in *N*,*N*-dimethylacetamide (DMA) formed a clear solution, but the fluorescence maximal intensity was very weak comparing with that in buffer (Fig. 2a and Fig. S3). The enzyme quenching might explain the CALB activity in DMA was about 3-fold lower than that in *t*-butanol (Table 1).

In hydrophobic ILs (containing anions of Tf_2N^-, PF_6^- or $beti^-$), aqueous droplets (10 μL, 20 mg/mL CALB) of CALB were dispersed into fine droplets rather than fully solubilized in the media (1.0 mL); therefore, the change in maximal intensity of fluorescence in hydrophobic ILs is not an absolute indication of protein denaturation. In the case of even more hydrophobic [$CH_3OCH_2CH_2PBu_3$][beti] (Fig. S11), the aqueous droplets of CALB were barely dispersed in the IL and no CALB emission peak could be detected. On the other hand, the water droplets of CALB become soluble in hydrophilic ILs, forming a 'homogeneous' solution. The addition of aqueous lipase droplets (10 μL) instead of the enzyme power into the solvent was based on several considerations: (1) after adding the droplets, the overall water content in the solvent was 1% (v/v) which had minimum influence on the medium environment; (2) water droplets can be better dispersed in hydrophobic media (into tiny droplets) than the enzyme powder since the enzyme is not soluble in hydrophobic solvents; (3) the final CALB concentration in the solvent was 0.2 mg/mL; such a low concentration could be achieved more uniformly and easily by adding the aqueous droplets than adding the powder. As illustrated in Fig. 2a, the maximum emission occurred at 305 nm for CALB in [BMIM][Tf_2N] (also in Fig. S4), and at 300 nm in [BMIM][PF_6] (Fig. S5), both of which showed blue shifts comparing with that (313 nm) in buffer. However, no apparent emission peak was seen for CALB in [BMIM][BF_4] (Fig. S6) and [BMIM][dca] (Fig. S7). This explained the relatively high lipase activities in [BMIM][Tf_2N]and [BMIM][PF_6], but an extremely low activity in [BMIM][dca] (see Table 1). It remains a mystery that fluorescence signal of CALB was completely quenched in [BMIM][BF_4] although the enzyme was still active in this IL (Table 1). Fig. 2b compares the emission spectra of CALB in [$CH_3OCH_2CH_2PBu_3$][Tf_2N] and [$CH_3OCH_2CH_2PBu_3$]Br with CALB in buffer. It is clear that CALB in [$CH_3OCH_2CH_2PBu_3$][Tf_2N] showed the characteristic peak at 314 nm, while the lipase in [$CH_3OCH_2CH_2PBu_3$]Br showed a red-shifted peak at 325 nm, implying the former IL is more protein-stabilizing than the bromide type. The fluorescence intensity is lowest in [$CH_3OCH_2CH_2PBu_3$][Tf_2N] due to the poor miscibility of aqueous CALB in the IL (while aqueous CALB is miscible in hydrophilic [$CH_3OCH_2CH_2PBu_3$]Br). Fig. 2c demonstrates the influence of different cation cores on the emission signal of CALB. Comparing with the emission peak of CALB in buffer at 313 nm, the red shifts of emission wavelength in different ILs increase in the order of [$CH_3OCH_2CH_2PBu_3$][Tf_2N] (314 nm), [$CH_3OCH_2CH_2PEt_3$][Tf_2N] (314 nm) < [$CH_3OCH_2CH_2SMe_2$][Tf_2N] (322 nm) < [$CH_3OCH_2CH_2$-Et_3N][Tf_2N] (329 nm) < [$CH_3OCH_2CH_2Py$][Tf_2N] (338 nm) < [$CH_3OCH_2CH_2$-Im-Et][Tf_2N] (344 nm) < [$CH_3OCH_2CH_2$-Pip-Me][Tf_2N] (no maximum). It is known that the solvent properties (such as polarity)

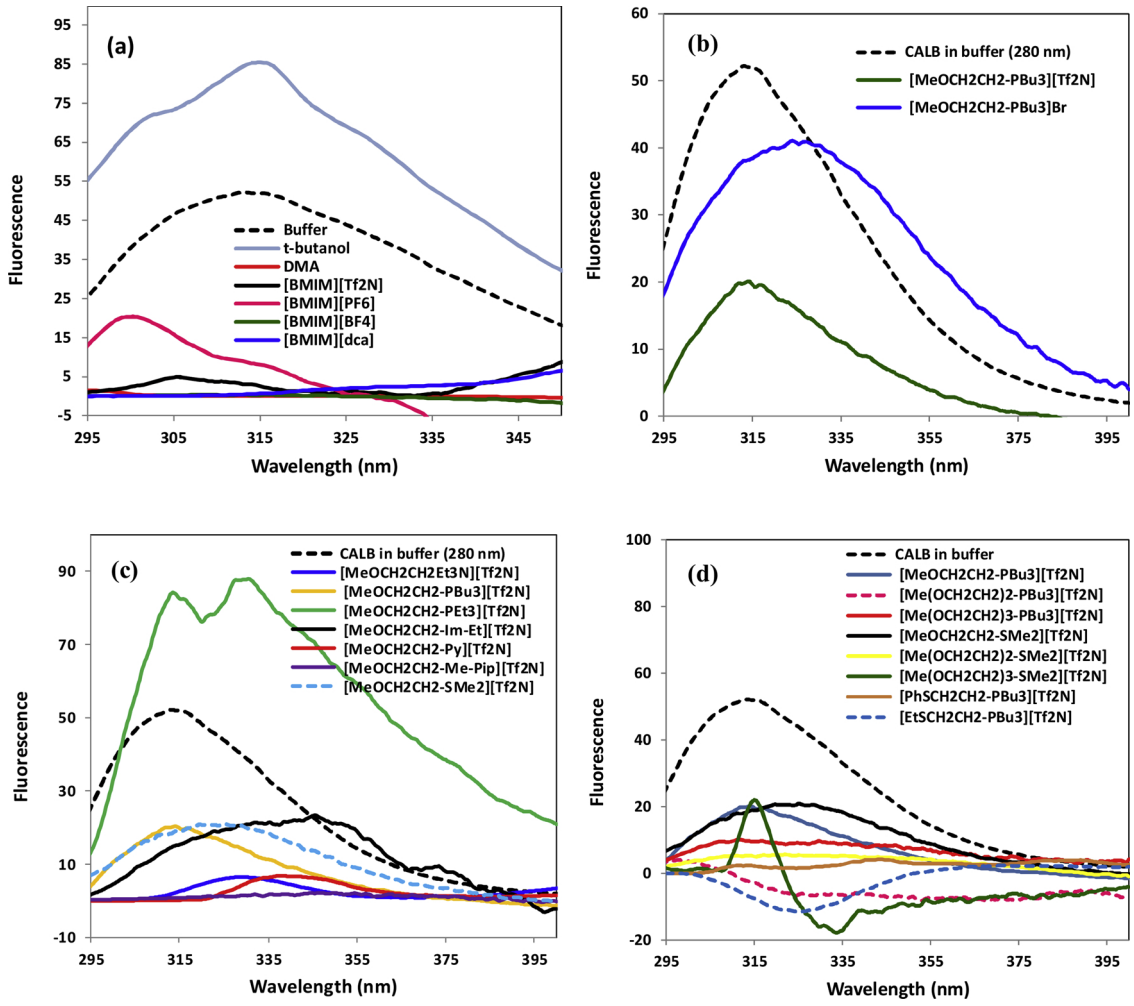

Fig. 2. Fluorescence emission spectra of CALB in different solvents (the solvent emission spectra were subtracted).

have a major impact on the tryptophan emission spectra and excited-state ionization of tyrosine [61,64]. This order is not always consistent with the CALB's transesterification activities at 50 °C shown in Table 1: $[CH_3OCH_2CH_2NEt_3][Tf_2N]$ > $[CH_3OCH_2CH_2Py][Tf_2N]$ > $[CH_3OCH_2CH_2PEt_3][Tf_2N]$ > $[CH_3OCH_2CH_2$-Pip-Me$][Tf_2N]$, $[CH_3OCH_2CH_2SMe_2][Tf_2N]$ > $[CH_3OCH_2CH_2$-Im-Et$][Tf_2N]$ > $[CH_3OCH_2CH_2PBu_3][Tf_2N]$. The lipase activities at 70 °C for the ROP of ε-caprolactone (in terms of M_w as discussed in Section 3.2) followed another sequence: $[CH_3OCH_2CH_2PBu_3][Tf_2N]$ > $[CH_3OCH_2CH_2$-Pip-Me$][Tf_2N]$ > $[CH_3OCH_2CH_2PEt_3][Tf_2N]$ > $[CH_3OCH_2CH_2Py][Tf_2N]$, $[CH_3OCH_2CH_2SMe_2][Tf_2N]$ > $[CH_3OCH_2CH_2$-Im-Et$][Tf_2N]$. Therefore, the lipase activity is also dependent on the specific substrates and different reaction conditions.

Fig. 2d suggests that a longer ethoxy chain attached to phosphonium leads to diminishing characteristic emission peak, which correlates well with lower CALB activities in $[CH_3(OCH_2CH_2)_2PBu_3][Tf_2N]$ and $[CH_3(OCH_2CH_2)_3PBu_3][Tf_2N]$ (trials 10 and 11 respectively in Table 1). The sulfonium ILs showed a different trend: $[CH_3(OCH_2CH_2)_3SMe_2][Tf_2N]$ showed a strong emission peak at 315 nm (Fig. S22), which correlates with a high CALB activity (trial 21 in Table 1). Two thioether-substituted phosphoniums $[PhSCH_2CH_2PBu_3][Tf_2N]$ and $[CH_3CH_2SCH_2CH_2PBu_3][Tf_2N]$ showed weak or no emission peak (Figs. 2d, S14 and S15), which explained the very low Novozym 435 activities in Table 1 (trials 22 and 23 respectively). However, the enzymatic ROP reaction in $[PhSCH_2CH_2PBu_3][Tf_2N]$ still produced poly(ε-caprolactone) with M_w 21,500 Da and 56% yield (trial 16 in Table 2), implying the substrate might provide some protective role for the lipase.

4. Conclusions

Ether-functionalized ILs with different cation cores have been synthesized and evaluated as solvents for two enzymatic reactions: the transesterification of ethyl sorbate and 1-propanol, and the ring-opening polymerization (ROP) of ε-caprolactone. Two ILs, $[CH_3OCH_2CH_2$-Et$_3$N$][Tf_2N]$ and $[CH_3OCH_2CH_2$-Py$][Tf_2N]$ afforded the highest transesterification reaction rates (> 6.0 μmol min^{-1} g^{-1} CALB) among all ILs studied. $[CH_3OCH_2CH_2$-PBu$_3][Tf_2N]$ produced the highest molecular mass (M_w up to 25,400 Da) in the polymerization reaction. We obtained different enzyme activity sequences for these two reactions, implying that the lipase activity depends on both the solvent and the specific reaction. The thermal stability of Novozym 435 in $[CH_3OCH_2CH_2$-Et$_3$N$][Tf_2N]$ is much higher than that in *t*-butanol. The fluorescence spectra of free CALB in different ILs allow a more insightful view of the interactions between the lipase and the solvent. The red shifts of emission wavelength in different ILs increase in the order of $[CH_3OCH_2CH_2PBu_3][Tf_2N]$ (314 nm), $[CH_3OCH_2CH_2PEt_3][Tf_2N]$ (314 nm) < $[CH_3OCH_2CH_2SMe_2][Tf_2N]$ (322 nm) < $[CH_3OCH_2CH_2$-Et$_3$N$][Tf_2N]$ (329 nm) < $[CH_3OCH_2CH_2Py][Tf_2N]$ (338 nm) < $[CH_3OCH_2CH_2$-Im-Et$][Tf_2N]$ (344 nm) < $[CH_3OCH_2CH_2$-Pip-Me$][Tf_2N]$ (no maximum). The solvent properties (such as polarity) and/or the lipase-solvent interactions could lead to the red shifts. Therefore, ether-functionalized ILs can be custom-designed for individual biocatalytic reactions.

Declarations of interest

None.

Acknowledgement

H. Z. acknowledges the startup fund support from the University of Northern Colorado.

Appendix A. Supplementary data

Supplementary material related to this article can be found, in the online version, at doi:https://doi.org/10.1016/j.procbio.2019.03.018.

References

[1] P.J. Halling, Biocatalysis in low-water media: understanding effects of reaction conditions, Curr. Opin. Chem. Biol. 4 (2000) 74–80.
[2] S. Cantone, U. Hanefeld, A. Basso, Biocatalysis in non-conventional media—ionic liquids, supercritical fluids and the gas phase, Green Chem. 9 (2007) 954–971, https://doi.org/10.1039/B618893A.
[3] J. Kadokawa, S. Kobayashi, Polymer synthesis by enzymatic catalysis, Curr. Opin. Chem. Biol. 14 (2010) 145–153, https://doi.org/10.1016/j.cbpa.2009.11.020.
[4] A. Zaks, A.M. Klibanov, Enzymatic catalysis in nonaqueous solvents, J. Biol. Chem. 263 (1988) 3194–3201.
[5] A.M. Klibanov, Why are enzymes less active in organic solvents than in water? Trends Biotechnol. 15 (1997) 97–101, https://doi.org/10.1016/S0167-7799(97)01013-5.
[6] F. van Rantwijk, R.A. Sheldon, Biocatalysis in ionic liquids, Chem. Rev. 107 (2007) 2757–2785, https://doi.org/10.1021/cr050946x.
[7] Z. Yang, W. Pan, Ionic liquids: green solvents for nonaqueous biocatalysis, Enzyme Microbial Technol. 37 (2005) 19–28, https://doi.org/10.1016/j.enzmictec.2005.02.014.
[8] P. Domínguez de María, Z. Maugeri, Ionic liquids in biotransformations: from proof-of-concept to emerging deep-eutectic-solvents, Curr. Opin. Chem. Biol. 15 (2011) 220–225, https://doi.org/10.1016/j.cbpa.2010.11.008.
[9] M. Moniruzzaman, K. Nakashima, N. Kamiya, M. Goto, Recent advances of enzymatic reactions in ionic liquids, Biochem. Eng. J. 48 (2010) 295–314, https://doi.org/10.1016/j.bej.2009.10.002.
[10] H. Zhao, Methods for stabilizing and activating enzymes in ionic liquids — a review, J. Chem. Tech. Biotechnol. 85 (2010) 891–907, https://doi.org/10.1002/jctb.2375.
[11] H. Zhao, Protein stabilization and enzyme activation in ionic liquids: specific ion effects, J. Chem. Technol. Biotechnol. 91 (2016) 25–50, https://doi.org/10.1002/jctb.4837.
[12] Z. Guo, X. Xu, New opportunity for enzymatic modification of fats and oils with industrial potentials, Org. Biomol. Chem. 3 (2005) 2615–2619, https://doi.org/10.1039/B506763D.
[13] Z. Guo, B. Chen, R.L. Murillo, T. Tan, X. Xu, Functional dependency of structures of ionic liquids: do substituents govern the selectivity of enzymatic glycerolysis? Org. Biomol. Chem. 4 (2006) 2772–2776, https://doi.org/10.1039/b606900b.
[14] Z. Guo, X. Xu, Lipase-catalyzed glycerolysis of fats and oils in ionic liquids: a further study on the reaction system, Green Chem. 8 (2006) 54–62, https://doi.org/10.1039/B511117J.
[15] B. Chen, Z. Guo, T. Tan, X. Xu, Structures of ionic liquids dictate the conversion and selectivity of enzymatic glycerolysis: theoretical characterization by COSMO-RS, Biotechnol. Bioeng. 99 (2008) 18–29, https://doi.org/10.1002/bit.21520.
[16] D. Kahveci, Z. Guo, B. Özçelik, X. Xu, Lipase-catalyzed glycerolysis in ionic liquids directed towards diglyceride synthesis, Process Biochem. 44 (2009) 1358–1365, https://doi.org/10.1016/j.procbio.2009.07.009.
[17] Z. Guo, D. Kahveci, B. Özçelik, X. Xu, Improving enzymatic production of diglycerides by engineering binary ionic liquid medium system, New Biotechnol. 26 (2009) 37–43, https://doi.org/10.1016/j.nbt.2009.04.001.
[18] D. Kahveci, Z. Guo, B. Özçelik, X. Xu, Optimisation of enzymatic synthesis of diacylglycerols in binary medium systems containing ionic liquids, Food Chem. 119 (2010) 880–885, https://doi.org/10.1016/j.foodchem.2009.07.040.
[19] T. De Diego, P. Lozano, M.A. Abad, K. Steffensky, M. Vaultier, J.L. Iborra, On the nature of ionic liquids and their effects on lipases that catalyze ester synthesis, J. Biotechnol. 140 (2009) 234–241, https://doi.org/10.1016/j.jbiotec.2009.01.012.
[20] G. de Gonzalo, I. Lavandera, K. Durchschein, D. Wurm, K. Faber, W. Kroutil, Asymmetric biocatalytic reduction of ketones using hydroxy-functionalised water-miscible ionic liquids as solvents, Tetrahedron Asymmetry 18 (2007) 2541–2546, https://doi.org/10.1016/j.tetasy.2007.10.010.
[21] S. Dreyer, U. Kragl, Ionic liquids for aqueous two-phase extraction and stabilization of enzymes, Biotechnol. Bioeng. 99 (2008) 1416–1424, https://doi.org/10.1002/bit.21720.
[22] D. Das, A. Dasgupta, P.K. Das, Improved activity of horseradish peroxidase (HRP) in 'specifically designed' ionic liquid, Tetrahedron Lett. 48 (2007) 5635–5639, https://doi.org/10.1016/j.tetlet.2007.06.022.
[23] Y. Abe, K. Kude, S. Hayase, M. Kawatsura, K. Tsunashima, T. Itoh, Design of phosphonium ionic liquids for lipase-catalyzed transesterification, J. Mol. Catal., B Enzym. 51 (2008) 81–85, https://doi.org/10.1016/j.molcatb.2007.11.010.
[24] C. Vafiadi, E. Topakas, V.R. Nahmias, C.B. Faulds, P. Christakopoulos, Feruloyl esterase-catalysed synthesis of glycerol sinapate using ionic liquids mixtures, J. Biotechnol. 139 (2009) 124–129, https://doi.org/10.1016/j.jbiotec.2008.08.008.
[25] H. Zhou, J. Chen, L. Ye, H. Lin, Y. Yuan, Enhanced performance of lipase-catalyzed kinetic resolution of secondary alcohols in monoether-functionalized ionic liquids, Bioresour. Technol. 102 (2011) 5562–5566, https://doi.org/10.1016/j.biortech.2011.02.066.
[26] Y. Fan, X. Wang, L. Zhang, J. Li, L. Yang, P. Gao, Z. Zhou, Lipase-catalyzed synthesis of biodiesel in a hydroxyl-functionalized ionic liquid, Chem. Eng. Res. Des. 132 (2018) 199–207, https://doi.org/10.1016/j.cherd.2018.01.020.
[27] Y. Fan, D. Cai, X. Wang, L. Yang, Ionic liquids: efficient media for the lipase-catalyzed Michael addition, Molecules 23 (2018) 2154, https://doi.org/10.3390/molecules23092154.
[28] S. Kadotani, T. Nokami, T. Itoh, Enhanced activity and modified substrate-favoritism of *Burkholderia cepacia* lipase by the treatment with a pyridinium alkyl-PEG sulfate ionic liquid, Tetrahedron 75 (2019) 441–447, https://doi.org/10.1016/j.tet.2018.12.028.
[29] H. Zhao, G.A. Baker, Z. Song, O. Olubajo, T. Crittle, D. Peters, Designing enzyme-compatible ionic liquids that can dissolve carbohydrates, Green Chem. 10 (2008) 696–705, https://doi.org/10.1039/B801489B.
[30] S. Tang, G.A. Baker, S. Ravula, J.E. Jones, H. Zhao, PEG-functionalized ionic liquids for cellulose dissolution and saccharification, Green Chem. 14 (2012) 2922–2932, https://doi.org/10.1039/C2GC35631G.
[31] H. Zhao, C.L. Jones, J.V. Cowins, Lipase dissolution and stabilization in ether-functionalized ionic liquids, Green Chem. 11 (2009) 1128–1138, https://doi.org/10.1039/B905388C.
[32] H. Zhao, Z. Song, Migration of reactive trace compounds from Novozym® 435 into organic solvents and ionic liquids, Biochem. Eng. J. 49 (2010) 113–118, https://doi.org/10.1016/j.bej.2009.12.004.
[33] H. Zhao, Z. Song, O. Olubajo, High transesterification activities of immobilized proteases in new ether-functionalized ionic liquids, Biotechnol. Lett. 32 (2010) 1109–1116, https://doi.org/10.1007/s10529-010-0262-4.
[34] H. Zhao, L.O. Afriyie, N.E. Larm, G.A. Baker, Glycol-functionalized ionic liquids for hight-emperature enzymatic ring-opening polymerization, RSC Adv. 8 (2018) 36025–36033, https://doi.org/10.1039/c8ra07733a.
[35] E. Coadou, P. Goodrich, A.R. Neale, L. Timperman, C. Hardacre, J. Jacquemin, M. Anouti, Synthesis and thermophysical properties of ether-functionalized sulfonium ionic liquids as potential electrolytes for electrochemical applications, ChemPhysChem 17 (2016) 3992–4002, https://doi.org/10.1002/cphc.201600882.
[36] U. Piotrowska, M. Sobczak, E. Oledzka, C. Combes, Effect of ionic liquids on the structural, thermal, and *in vitro* degradation properties of poly(ε-caprolactone) synthesized in the presence of *Candida antarctica* lipase B, J. Appl. Polym. Sci. 133 (2016) 43728, https://doi.org/10.1002/app.43728.
[37] M. Mena, A. López-Luna, K. Shirai, A. Tecante, M. Gimeno, E. Bárzana, Lipase-catalyzed synthesis of hyperbranched poly-L-lactide in an ionic liquid, Bioprocess Biosyst. Eng. 36 (2013) 383–387, https://doi.org/10.1007/s00449-012-0792-3.
[38] D. Omay, Y. Guvenilir, Synthesis and characterization of poly(D,L-lactic acid) via enzymatic ring opening polymerization by using free and immobilized lipase, Biocatal. Biotransform. 31 (2013) 132–140, https://doi.org/10.3109/10242422.2013.795148.
[39] J.R. Rumble, CRC Handbook of Chemistry and Physics, 99th ed., CRC Press, Taylor & Francis Group, New York, 2018.
[40] H. Zhao, G.A. Baker, S. Holmes, New eutectic ionic liquids for lipase activation and enzymatic preparation of biodiesel, Org. Biomol. Chem. 9 (2011) 1908–1916, https://doi.org/10.1039/c0ob01011a.
[41] F.C. Loeker, C.J. Duxbury, R. Kumar, W. Gao, R.A. Gross, S.M. Howdle, Enzyme-catalyzed ring-opening polymerization of ε-caprolactone in supercritical carbon dioxide, Macromolecules 37 (2004) 2450–2453, https://doi.org/10.1021/ma0349884.
[42] F. Deng, R.A. Gross, Ring-opening bulk polymerization of ε-caprolactone and trimethylene carbonate catalyzed by lipase Novozym 435, Int. J. Biol. Macromol. 25 (1999) 153–159, https://doi.org/10.1016/S0141-8130(99)00029-X.
[43] A.R. Toral, A.P. de los Ríos, F.J. Hernández, M.H.A. Janssen, R. Schoevaart, F. van Rantwijk, R.A. Sheldon, Cross-linked *Candida antarctica* lipase B is active in denaturing ionic liquids, Enzyme Microb. Technol. 40 (2007) 1095–1099.
[44] S. Tang, G.A. Baker, H. Zhao, Ether- and alcohol-functionalized task-specific ionic liquids: attractive properties and applications, Chem. Soc. Rev. 41 (2012) 4030–4066, https://doi.org/10.1039/C2CS15362A.
[45] H. Zhao, G.A. Nathaniel, P.C. Merenini, Enzymatic ring-opening polymerization (ROP) of lactides and lactone in ionic liquids and organic solvents: digging the controlling factors, RSC Adv. 7 (2017) 48639–48648, https://doi.org/10.1039/c7ra09038b.
[46] S. Kobayashi, K. Takeya, S. Sudu, H. Uyama, Lipase-catalyzed ring-opening polymerization of medium-size lactones to polyesters, Macromol. Chem. Phys. 199 (1998) 1729–1736.
[47] R. Marcilla, M. de Geus, D. Mecerreyes, C.J. Duxbury, C.E. Koning, A. Heise, Enzymatic polyester synthesis in ionic liquids, Eur. Polym. J. 42 (2006) 1215–1221, https://doi.org/10.1016/j.eurpolymj.2005.12.021.
[48] C. Wu, Z. Zhang, C. Chen, F. He, R. Zhuo, Synthesis of poly(ε-caprolactone) by an immobilized lipase coated with ionic liquids in a solvent-free condition, Biotechnol. Lett. 35 (2013) 1623–1630, https://doi.org/10.1007/s10529-013-1245-z.
[49] A. Duda, A. Kowalski, S. Penczek, H. Uyama, S. Kobayashi, Kinetics of the ring-opening polymerization of 6-, 7-, 9-, 12-, 13-, 16-, and 17-membered lactones. Comparison of chemical and enzymatic polymerizations, Macromolecules 35 (2002) 4266–4270, https://doi.org/10.1021/ma012207y.
[50] A. Kumar, R.A. Gross, *Candida antartica* lipase B catalyzed polycaprolactone

synthesis: effects of organic media and temperature, Biomacromolecules 1 (2000) 133–138, https://doi.org/10.1021/bm990510p.
[51] L.A. Henderson, Y.Y. Svirkin, R.A. Gross, D.L. Kaplan, G. Swift, Enzyme-catalyzed polymerizations of ε-caprolactone: effects of initiator on product structure, propagation kinetics, and mechanism, Macromolecules 29 (1996) 7759–7766.
[52] P. Lozano, T. De Diego, D. Carrié, M. Vaultier, J.L. Iborra, Over-stabilization of *Candida antarctica* lipase B by ionic liquids in ester synthesis, Biotechnol. Lett. 23 (2001) 1529–1533.
[53] P. Lozano, T. de Diego, D. Carrie, M. Vaultier, J.L. Iborra, Enzymatic ester synthesis in ionic liquids, J. Mol. Catalysis B: Enzym. 21 (2003) 9–13.
[54] P. Lozano, T. de Diego, J.-P. Guegan, M. Vaultier, J.L. Iborra, Stabilization of α-chymotrypsin by ionic liquids in transesterification reactions, Biotechnol. Bioeng. 75 (2001) 563–569.
[55] O. Ulbert, K. Bélafi-Bakó, K. Tonova, L. Gubicza, Thermal stability enhancement of *Candida rugosa* lipase using ionic liquids, Biocatalysis Biotransform. 23 (2005) 177–183.
[56] H. Noritomi, K. Minamisawa, R. Kamiya, S. Kato, Thermal stability of proteins in the presence of aprotic ionic liquids, J. Biomed. Sci. Eng. 4 (2011) 94–99, https://doi.org/10.4236/jbise.2011.42013.
[57] H.J. Park, K. Park, Y.J. Yoo, Understanding the effect of *tert*-butanol on *Candida antarctica* lipase B using molecular dynamics simulations, Mol. Simul. 39 (2013) 653–659, https://doi.org/10.1080/08927022.2012.758850.
[58] J. Uppenberg, M.T. Hansen, S. Patkar, T.A. Jones, The sequence, crystal structure determination and refinement of two crystal forms of lipase B from *Candida antarctica*, Structure 2 (1994) 293–308.
[59] J. Uppenberg, N. Oehrner, M. Norin, K. Hult, G.J. Kleywegt, S. Patkar, V. Waagen, T. Anthonsen, T.A. Jones, Crystallographic and molecular-modeling studies of lipase B from *Candida antarctica* reveal a stereospecificity pocket for secondary alcohols, Biochemistry (Mosc). 34 (1995) 16838–16851.
[60] B. Réjasse, T. Besson, M.-D. Legoy, S. Lamare, Influence of microwave radiation on free *Candida antarctica* lipase B activity and stability, Org. Biomol. Chem. 4 (2006) 3703–3707.
[61] J.R. Lakowicz, 16. Protein fluorescence, Principles of Fluorescence Spectroscopy, 3rd ed., Springer, New York, 2006.
[62] P. Lozano, T. De Diego, J.L. Iborra, Dynamic structure/function relationships in the α-chymotrypsin deactivation process by heat and pH, Eur. J. Biochem. 248 (1997) 80–85, https://doi.org/10.1111/j.1432-1033.1997.00080.x.
[63] Y. Chen, Z. Chen, J. Yang, J. Jin, J. Zhang, R. Yu, Quantitative fluorescence spectroscopy in turbid media: a practical solution to the problem of scattering and absorption, Anal. Chem. 85 (2013) 2015–2020, https://doi.org/10.1021/ac302815e.
[64] A.S. Ladokhin, Fluorescence spectroscopy in peptide and protein analysis, in: R.A. Meyers (Ed.), Encyclopedia of Analytical Chemistry, John Wiley & Sons Ltd, Chichester, 2000, pp. 5762–5779.
[65] K.R. Harris, M. Kanakubo, L.A. Woolf, Temperature and pressure dependence of the viscosity of the ionic liquid 1-butyl-3-methylimidazolium tetrafluoroborate: viscosity and density relationships in ionic liquids, J. Chem. Eng. Data 52 (2007) 2425–2430, https://doi.org/10.1021/je700370z.
[66] P.J. Carvalho, T. Regueira, L.M.N.B.F. Santos, J. Fernandez, J.A.P. Coutinho, Effect of water on the viscosities and densities of 1-butyl-3-methylimidazolium dicyanamide and 1-butyl-3-methylimidazolium tricyanomethane at atmospheric pressure, J. Chem. Eng. Data 55 (2010) 645–652, https://doi.org/10.1021/je900632q.